Proc. Natl. Acad. Sci. USA
Vol. 95, pp. 5795–5800, May 1998
Neurobiology

Amyloid β-peptide stimulates nitric oxide production in astrocytes through an NFκB-dependent mechanism

KEITH T. AKAMA†, CHRIS ALBANESE‡, RICHARD G. PESTELL‡, AND LINDA J. VAN ELDIK†§¶

†Department of Cell and Molecular Biology and §Northwestern Drug Discovery Program, Northwestern University Medical School, Chicago, IL 60611-3008; and ‡Department of Medicine and Developmental and Molecular Biology, Albert Einstein College of Medicine, Bronx, NY 10461

Communicated by Laslo Lorand, Northwestern University Medical School, Chicago, IL, February 26, 1998 (received for review December 29, 1997)

ABSTRACT **The major pathological features of Alzheimer's disease (AD) include amyloid plaques composed primarily of the β-amyloid (Aβ) peptide, degenerating neurons and neurofibrillary tangles, and the presence of numerous activated astrocytes and microglia. Although extensive genetic data implicate Aβ in the neurodegenerative cascade of AD, the molecular mechanisms underlying its effects on neurons and glia and the relationship between glial activation and neuronal death are not well defined. Aβ has been shown to induce glial activation, and a growing body of evidence suggests that activated glia contribute to neurotoxicity through generation of inflammatory cytokines and neurotoxic free radicals, such as nitric oxide (NO), potent sources of oxidative stress known to occur in AD. It is therefore crucial to identify specific Aβ-induced molecular pathways mediating these responses in activated glia. We report that Aβ stimulates the activation of the transcription factor NFκB in rat astrocytes, that NFκB activation occurs selectively from p65 transactivation domain 2, and that Aβ-induced NO synthase expression and NO production occur through an NFκB-dependent mechanism. This demonstration of how Aβ couples an intracellular signal transduction pathway involving NFκB to a potentially neurotoxic response provides a key mechanistic link between Aβ and the generation of oxidative damage. Our results also suggest possible molecular targets upon which to focus future drug discovery efforts for AD.**

Alzheimer's disease (AD) is a neurodegenerative disorder resulting in progressive neuronal death and memory loss. Neuropathologically, the disease is characterized by neurofibrillary tangles and neuritic plaques composed of aggregates of β-amyloid (Aβ) protein, a 40–43 amino acid proteolytic fragment derived from the amyloid precursor protein. The importance of Aβ in AD has been shown by means of several transgenic animal studies. The overexpression of mutant amyloid precursor protein results in neuritic plaque formation and synapse loss (1) and correlative memory deficits, as well as behavioral and pathological abnormalities similar to those found in AD (2).

Neuritic plaques in AD are densely surrounded by reactive astrocytes (3, 4). These reactive astrocytes participate in the inflammatory response observed in AD by their production of proinflammatory cytokines such as interleukin 1β (5), and by their expression of inducible nitric oxide synthase (iNOS) (6, 7). iNOS generates nitric oxide (NO) and NO-derived reactive nitrogen species such as peroxynitrite. One possible pathology of AD therefore can be viewed as the accumulation of such free radicals during inflammation resulting in lipid peroxidation, tyrosine nitrosylation, DNA oxidative damage, and ultimately neuronal destruction within the brain (8–11). Understanding the expression of iNOS in the AD brain is therefore critical. NOS immunoreactivity has been observed near Aβ neuritic plaques (7), and iNOS expression can be stimulated in cultured astrocytes or microglia by Aβ (6, 12–15). This Aβ stimulation of iNOS can result in the production of excessive amounts of diffusible NO, which when converted to peroxynitrite, becomes a powerfully detrimental oxidant with direct cytopathological consequences (16).

Relatively little is known about the molecular mechanisms governing Aβ stimulation of astrocyte iNOS activity. One candidate pathway involves the transcription factor NFκB (17). NFκB is a heterodimeric transcription factor composed of subunits from the Rel family of proteins. It is located in the cytoplasm as an inactive complex when associated with its inhibitor IκB, which masks the NFκB nuclear localization signal. Upon stimulation by cytokines or cellular stress, NFκB can be rapidly activated by the phosphorylation of IκB at serine residues, which direct IκB for proteosome-mediated degradation (18). The activated NFκB heterodimer is then free to translocate into the nucleus and bind to specific 10-bp response elements of target genes, typically found in inflammation-responsive genes. The iNOS promoter contains at least one NFκB response element (19), and activated NFκB is an important transcription factor in iNOS gene expression in response to cytokines or cellular stress (20). Recently, NFκB was observed immunohistochemically in postmortem AD brain (21).

We report here that Aβ activates NFκB in cultured rat astrocytes and demonstrate that Aβ stimulation of iNOS expression and NO production occurs through an NFκB-dependent mechanism. These data define a specific molecular pathway that links Aβ activation of glia to a potentially neurotoxic oxidative stress response, and support the concept that Aβ-induced oxidative damage is neuropathogenic in AD.

MATERIALS AND METHODS

Cell Culture and Amyloid β 1–42 Peptide (Aβ42) Preparation. Cultured rat cortical astrocytes were prepared and tertiary cultures made as described (22). Cells were maintained in αMEM supplemented with 10% fetal bovine serum (FBS) (HyClone) and antibiotics [100 units/ml penicillin/100 μg/ml streptomycin (GIBCO/BRL)]. Twenty-four hours before stimulation, astrocyte medium was removed, cells were washed once with prewarmed PBS, and then serum-free αMEM containing N2 media supplement (GIBCO/BRL) was added to the cultures. Aβ peptides [Aβ 1–42 or scrambled 1–42 sequence (Aβ42scr) KVKGLIDGAHIGDLVYEFMD-SNSAIFREGVGAGHVHVAQVEF] were either purchased

The publication costs of this article were defrayed in part by page charge payment. This article must therefore be hereby marked "*advertisement*" in accordance with 18 U.S.C. §1734 solely to indicate this fact.

Abbreviations: Aβ42, amyloid β 1–42 peptide; Aβ42scr, scrambled Aβ1–42 sequence; AD, Alzheimer's disease; EMSA, electrophoretic mobility-shift assay; iNOS, inducible nitric oxide synthase; TAD, transactivating domain; RLU, relative light unit.

¶To whom reprint requests should be addressed at: Northwestern University Medical School, W-129, 303 East Chicago Avenue, Chicago, IL 60611-3008. e-mail: vaneldik@nwu.edu.

(Bachem) or prepared as described previously (6). Aβ peptides were aggregated as described previously (6). Briefly, a 20× Aβ peptide stock was subjected to 2-day acidic aging conditions (200 μM Aβ in 1 mM HCl) at room temperature, or a 10× Aβ stock was subjected to 1-day neutral aging conditions (100 μM Aβ in αMEM/0.2% dimethyl sulfoxide) at 4°C. The aggregated Aβ stocks contained both fibrillar species and globular oligomeric aggregates by atomic force microscopy. The Aβ stocks were then added to the cultures at the appropriate stimulus concentration.

Electrophoretic Mobility-Shift Assays (EMSA). Nuclear extracts from treated astrocytes were prepared by a modified Dignam method (23). Briefly, treated cells (10^6 cells per 60-mm dish) were scraped into ice-cold PBS supplemented with 1 mM phenylmethylsulfonyl fluoride (PMSF). Cells were pelleted in microfuge tubes and resuspended in 400 μl of ice-cold low-salt buffer A (10 mM Hepes, pH 7.9/1.5 mM $MgCl_2$/10 mM KCl). After 10 min on ice, 25 μl of 10% Nonidet P-40 was added and the samples were vortexed vigorously for 10 sec. Samples were centrifuged (13,000 × *g*) for 30 sec at 4°C, and the pellet was resuspended in 30 μl of ice-cold high-salt buffer C (20 mM Hepes, pH 7.9)/25% glycerol/420 mM NaCl/1.5 mM $MgCl_2$/0.2 mM EDTA). Resuspended pellets were allowed to rock gently at 4°C for 30 min and then centrifuged at 4°C for 15 min. The supernatant (nuclear extract) was saved and protein concentration was determined by Bradford assay. Before using both buffer A and buffer C, a fresh mixture of inhibitors was added to each at a final concentration of 1 mM PMSF, 1 μg/ml leupeptin A, 1 mM DTT, and 1 mM sodium orthovanadate. Binding reactions were assayed in 20 μl volumes by incubating 3 μg of nuclear extract with reaction buffer [50 mM Tris·HCl, pH 7.5/5 mM EDTA/2.5 mM DTT/250 mM NaCl/0.25 mg/ml poly(dI·dC)·poly(dI·dC) (Pharmacia)]. For competition, unlabeled specific (identical NFκB oligonucleotide shift probe) or nonspecific (AP2 oligonucleotide shift probe) (Promega) probes were allowed to incubate with appropriate samples in 50-fold molar excess for 10–15 min before incubating all samples with ^{32}P-labeled oligonucleotide shift probes (approximately 50,000–200,000 cpm) at room temperature for 20 min. "Super-shifting" was conducted by then incubating the appropriate samples with Rel family antibodies (6 μg per sample) for 45 min at room temperature. Supershift polyclonal antibodies against synthetic peptides from the NFκB/Rel family of proteins p65(RelA), p50, p52, c-Rel(p75), and RelB(p68) were purchased from Santa Cruz Biotechnology. Products were subjected to electrophoresis at 200 V in a 4°C room for approximately 90 min on 5.5% nondenaturing polyacrylamide gels in high ionic strength TGE buffer (50 mM Tris·HCl/380 mM glycine/2 mM EDTA, pH ≈8.5). Lanes with samples were devoid of any loading dyes, which interfere with the binding reactions. Dried gels were exposed to Storm Phosphor Imaging plates (Molecular Dynamics) and viewed by IMAGEQUANT software (Molecular Dynamics). To size EMSA figures to page, the vertical aspect ratio of each picture was reduced by approximately 50%. Oligonucleotides representing the NFκB response element (consensus sequence, 5′-AGT TGA GGG GAC TTT CCC AGG C-3′) were purchased from Promega. Mutant NFκB (NFκBmut) response element oligonucleotides (5′-AGT TGA GGC* GAC TTT CCC AGG C-3′, where * denotes mutated base) were purchased from Santa Cruz Biotechnology. To prepare gel shift probes, oligonucleotides were labeled with [γ-^{32}P]ATP (Amersham) by using T4 polynucleotide kinase by the protocol provided (gel shift assay system, Promega). Unincorporated nucleotides were removed by Centri-Sep spin columns (Princeton Separations).

Plasmids. 3xRel-LUC was a gift from M. L. Scott and D. Baltimore (Massachusetts Institute of Technology) and contains three tandem Ig κB repeats from the construct −55 to +19 hIFNβ-CAT (24), which were cloned into the *Not*I–*Hin*dIII site of pBL, and thereby linked to the luciferase reporter gene. CMV-IκB(Super-repressor) [CMV-IκB(Sr)] was generously provided by Dean Ballard (Howard Hughes Medical Institute, Vanderbilt University Medical Center). IκB was cloned into the expression vector pCMV-4, and serine residues 32 and 36 (sites of phosphorylation that precede IκB degradation) have been mutated to alanines (25). pXP2 backbone vector and 7kb(wt) iNOS-LUC were kindly provided by David Geller (University of Pittsburgh) and have been described (26). PCR site-directed mutagenesis (QuikChange, Stratagene) was used to mutate the NFκB response element immediately upstream of the TATAA box of the 7kb(wt) iNOS-LUC promoter construct (GGG to CTC) to generate the 7kb(NFκB$^-$) iNOS-LUC promoter construct. DNA sequence analysis confirmed the mutation in the response element and verified the absence of any additional mutations. UAS(5x)-E1B-TATA-LUC (UAS-LUC) contains five tandem repeats of the Gal4 upstream activating sequence cloned pA3-LUC and has been described (27).

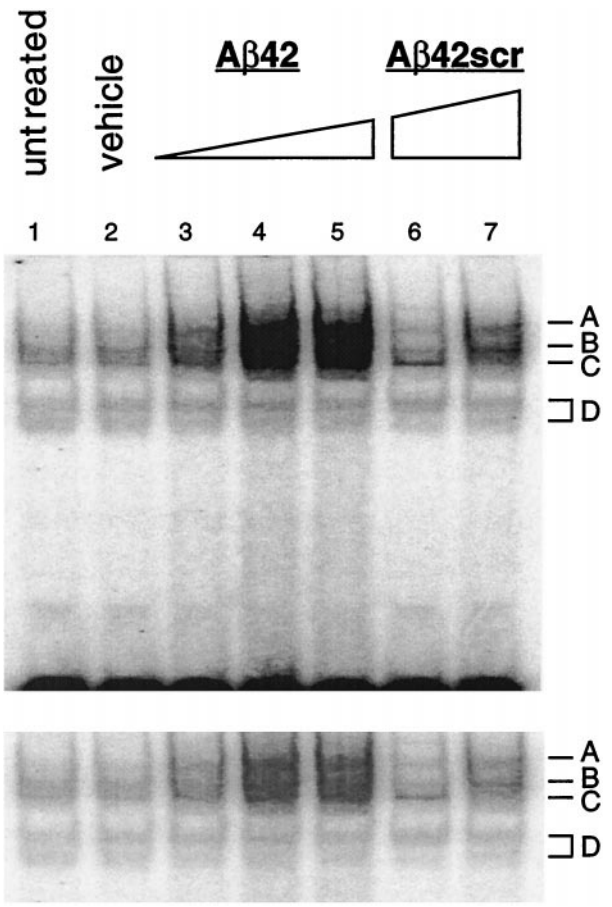

FIG. 1. Aβ42 activates NFκB in a dose-dependent manner. Nuclear extracts from astrocytes stimulated by increasing doses of Aβ42 were incubated with ^{32}P-labeled NFκB oligonucleotide probe for gel mobility-shift assay. Lanes: 1, untreated astrocyte nuclear extract; 2, vehicle-treated nuclear extract (0 μM Aβ42); 3–5, 1 μM, 5 μM, and 10 μM Aβ42, respectively. As a peptide control, nuclear extracts from astrocytes stimulated by a scrambled Aβ42 peptide [10 μM Aβ42scr (lane 6) and 20 μM Aβ42scr (lane 7)] were run to demonstrate the activation specificity of Aβ42. Cells were treated for 12 hr, a time-point where maximal NFκB activation could be detected by EMSA (data not shown). NFκB activation complexes are indicated by A–D. (*Lower*) A shorter exposure of the autoradiogram to allow better visualization of the individual complexes in lanes 4 and 5.

Transient Transfections. Astrocytes were transfected by using the synthetic cationic lipid Tfx-50 (Promega) or by SuperFect transfection reagent (Qiagen, Chatsworth, CA).

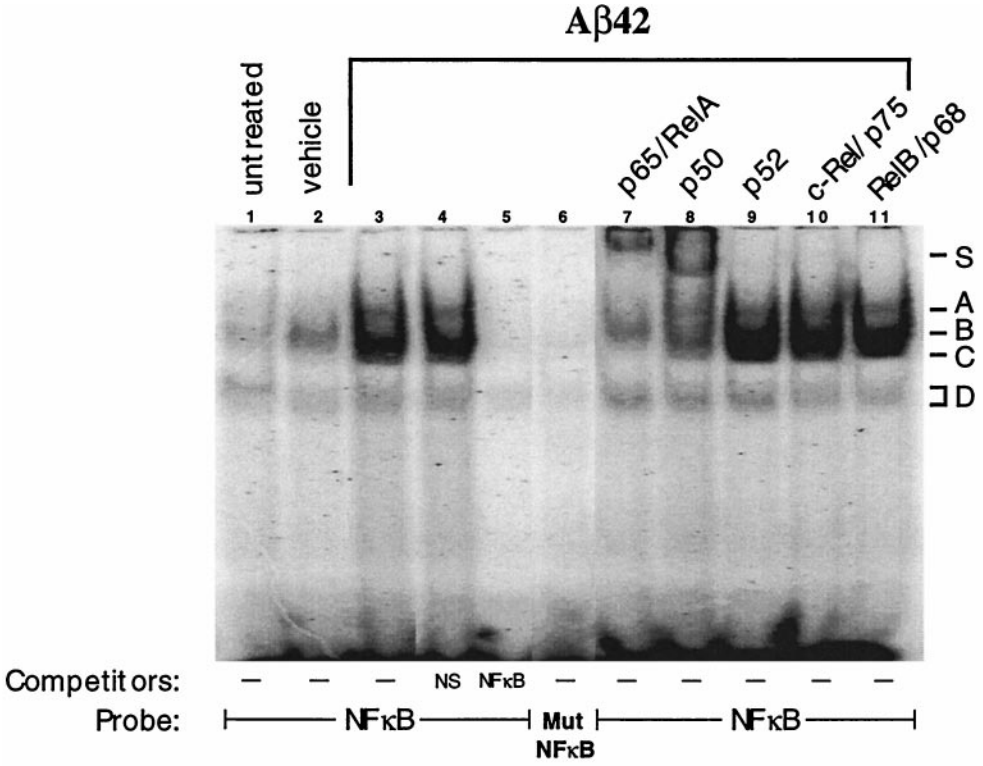

FIG. 2. Specificity of Aβ42-activated NFκB. Gel mobility-shift assay with nuclear extracts prepared from untreated astrocytes (lane 1), vehicle-control-treated astrocytes (lane 2), and 10 μM Aβ42-treated astrocytes (lanes 3–11). Cells were incubated for 12 hr. ^{32}P-labeled oligonucleotide shift probes used contained consensus NFκB response element (lanes 1–3 and 7–11), 50-fold molar excess of unlabeled AP2 (nonspecific competitor, NS) shift probe before ^{32}P-labeled NFκB shift probe (lane 4), approximately 50-fold molar excess of unlabeled NFκB (specific competitor, NFκB) shift probe before ^{32}P-labeled NFκB shift probe (lane 5), or ^{32}P-labeled mutant NFκB carrying a 1-bp substitution within the NFκB response element (lane 6). Polyclonal antibodies used to detect the indicated Rel family subunits are as indicated (lanes 7–11). NFκB activation complexes are indicated by A–D. Supershifted complexes are indicated by S and were detected only in samples incubated with either p65/RelA or p50 antibody.

Optimized DNA/reagent ratios were determined to be 1:1 (micrograms DNA/lipid charge) for Tfx-50, and 1:1 (micrograms DNA/microliters reagent) for SuperFect. All DNA used in transfections were prepared by the endotoxin-free plasmid prep (Endo-Free Maxi-prep kits, Qiagen). For transfections, secondary astrocytes were trypsinized and replated into 12-well or 48-well tissue culture plates (1.5×10^5 cells per well for 12-well plates, 1×10^4 cells per well for 48-well plates). Cells were immediately exposed to DNA transfecting complexes for 1–2 hr at 37°C. Transfecting complexes were then removed, cells washed once with warm PBS, and incubated for 4–6 hr in αMEM (with 20% FBS). This medium was then replaced with αMEM containing 10% FBS, and cells were incubated overnight before changing the medium to serum-free N2-supplemented αMEM for 24 hr before stimulation. For luciferase assays after the appropriate stimulus, cells were rinsed once with ice-cold PBS and immediately lysed for 5 min at 4°C in lysis buffer (0.5 M Hepes, pH 7.4/5% Triton N-101/1 mM $CaCl_2$/1 mM $MgCl_2$). Lysates were transferred to 96-well black-walled plates (Corning Costar), and an equal volume of reconstituted LucLite luciferase substrate (Packard) was added to each sample. Luciferase reactions were allowed to proceed for approximately 5 min at room temperature before quantitating relative light unit (RLU) output on a LumiCount (Packard) high-throughput luminometer (20-sec reads per sample well). Blank transfections (unstimulated astrocytes transfected with the appropriate backbone vector) were included for each experiment to determine machine noise background, which was then subtracted before data analysis. Each set of data represents results from 6–11 experiments.

Nitrite Assays. Nitrite production by astrocytes was measured by Griess assay as a read-out for iNOS activity as described previously (22). Astrocytes were treated with various stimuli in a total volume of 100 μl per well in a 48-well plate, and 80 μl of conditioned medium was collected after 48 hr of stimulus. To measure total nitrite produced in a 48-hr period, any nitrate in the conditioned medium was first reduced back to nitrite with nitrate reductase and NAPDH (Sigma) at 37°C for 1 hr. An equal volume of Griess reagent [0.5% sulfanilamide and 0.05% *N*-(1-naphthyl) ethylenediamine] was then added to the conditioned medium and the reaction was allowed to proceed for 5 min at room temperature before the absorbance at 540 nm was measured. A sodium nitrite linear range standard curve from 0 to 75 μM nitrite was used to determine the concentration of nitrite in the astrocyte conditioned medium.

RESULTS

To characterize the activation state of NFκB in astrocytes stimulated by Aβ42, we performed EMSA assays on isolated nuclear extracts incubated with ^{32}P-labeled oligonucleotide probes containing the 10-bp consensus sequence of the NFκB response element.

Four mobility-shifted complexes were observed using nuclear extracts from astrocytes treated with Aβ42 (Fig. 1, lanes 3, 4, and 5, bands A–D). Bands A, B, and C exhibited a dose-dependent increase in binding, beginning with nuclear extracts from cells treated with 1 μM Aβ42 (Fig. 1, lane 3). In contrast, nuclear extracts from cells treated with a scrambled Aβ42 peptide sequence (Aβ42scr) exhibited only a modest gel shift at double the maximum concentration of Aβ42 (Fig. 1, lane 7).

The specificity of the NFκB response was characterized further by EMSA. Compared with controls (Fig. 2, lanes 1 and 2), NFκB was strongly activated in astrocytes stimulated by Aβ42 (Fig. 2, lane 3). Maximal enhancement of binding was observed by 12 hr after Aβ activation (data not shown). All four bands could be competed away by specific competitor probe (50-fold molar excess of cold cognate competitor; Fig. 2, lane 5) but not by nonspecific probe (50-fold molar excess of unlabeled oligo shift probe containing the AP2 binding site; Fig. 2, lane 4). In addition, a mutant oligonucleotide probe that included a 1-bp substitution in the NFκB response element sequence exhibited little if any gel shift activity (Fig. 2, lane 6). Lysates from Aβ-activated astrocytes assayed by Western immunoblotting revealed the presence of all five protein members of the Rel family (data not shown). "Super-shifts," conducted with a panel of antibodies specific for each Rel family member, identified p65/RelA and p50 within the complex (Fig. 2, lanes 7–11). Bands A, B, and C were shifted by the antibodies to p65/RelA and p50, but not by the antibodies to p52, c-Rel/p75, or RelB/p68. Band D was unaffected by any of these Rel family antibodies.

The activation of NFκB was also determined by using the luciferase NFκB reporter construct 3xRel-LUC. This reporter construct has three tandem NFκB response element repeats upstream of a minimal promoter driving the luciferase gene.

Aβ42 treatment induced 3xRel-LUC approximately 4.5-fold over the levels in untreated or vehicle-treated cells (Fig. 3*A*). Aβ42scr did not stimulate 3xRel-LUC reporter expression levels above untreated or vehicle-treated cells (Fig. 3*A*). 3xRel-LUC reporter specificity for NFκB was verified by cotransfection with CMV-IκB(Sr), an IκB "super-repressor" expression construct. In this construct, IκB serines 32 and 36 have been mutated to alanines, preventing the protein from being phosphorylated, thereby blocking its degradation and thus strongly maintaining inhibition of NFκB activity. Overexpression of IκB(Sr) blocked Aβ42-dependent 3xRel-LUC activity to levels equivalent to unstimulated cells (Fig. 3*B*).

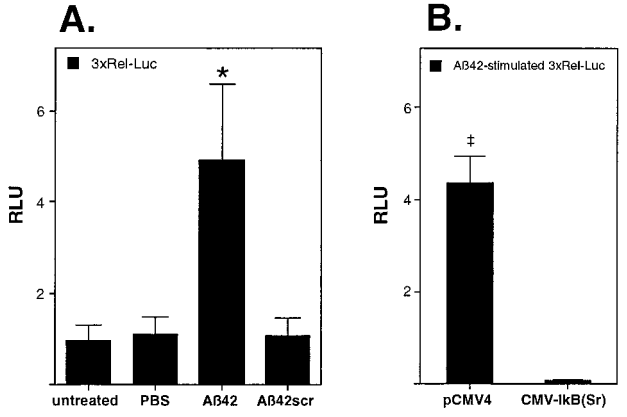

FIG. 3. Aβ42-specific stimulation of NFκB reporter gene activation. (*A*) The 3xRel-LUC plasmid (three tandem NFκB response element repeats with a minimal promoter cloned upstream of the luciferase gene) was transfected into astrocytes, which were then left untreated or stimulated for 12 hr by either PBS, 10 μM Aβ42, or 10 μM Aβ42scr. Luciferase expression in Aβ42-stimulated cells was significantly increased above that in untreated, PBS-treated, or Aβ42scr-treated cells. Data shown (mean ± SEM) represent $n = 8$ transfections and are RLUs. (*B*) Cotransfecting the 3xRel-LUC construct with the IκB (Super-repressor, Sr) expression construct [CMV-IκB(Sr)] reduced Aβ-stimulated 3xRel-LUC luciferase activity to near background levels compared with cotransfection of 3xRel-LUC with the backbone vector pCMV4. *, Significantly different from PBS control ($P < 0.05$); ‡, significantly different from control vector ($P < 0.005$). Statistics here and results throughout have been calculated by Student's *t* test. Significance is determined if $P < 0.05$.

Because p65/RelA was a participating subunit of NFκB, a subunit known to have at least two different transactivating domains (TADs) (28), we used two p65 TADs in yeast Gal4-dependent reporter constructs to determine which domain(s) specifically participated in Aβ42-stimulated NFκB activation. NFκB(1)-Gal4 included TAD1 of p65, which contains amino acid residues 520–590, and NFκB(2)-Gal4 included TAD2 of p65, which contains amino acid residues 286–518 (29). Either construct was cotransfected with a luciferase reporter construct containing five tandem repeats of the yeast Gal4-UAS binding site. As shown in Fig. 4, Aβ42 stimulated NFκB(2)-Gal4 2- to 3-fold, whereas cells transfected with NFkB(1)-Gal4 showed no induction. In addition, transfected cells treated with Aβ42scr showed no significant activity from either TAD1 or TAD2 of p65. Therefore, NFκB activation by Aβ42 is selectively regulated at the amino acid region of p65/RelA TAD 2.

We have previously shown that Aβ42 can enhance iNOS mRNA expression and nitrite production in cultured astrocytes (6). To characterize the potential importance of Aβ-activated NFκB for iNOS activity, we used several approaches. Astrocytes transfected with a human 7-kb iNOS promoter-luciferase construct [7kb(wt) iNOS-LUC] exhibited an approximate 7- to 10-fold increase in luciferase activity in Aβ42-activated astrocytes compared with vehicle-treated or untreated astrocytes (Fig. 5*A Left*). This Aβ-induced increase in iNOS promoter activity was almost completely abolished upon mutation of the proximal NFkB response element (5′-GGGACACTCC-3′ to 5′-CTCACACTCC 3′) (Fig. 5*A Right*). However, despite a reduction in basal level activity, the 7kb(NFκB$^-$) iNOS-LUC promoter construct responds to stimulation by 1 mM dibutyryl cAMP in a fashion indistinguishable to that of the 7kb(wt) iNOS-LUC construct (data not shown), demonstrating that NFκB-independent signaling pathways were unaffected by mutation of the NFκB binding site. Furthermore, cotransfection with CMV-IκB(Sr) abrogated Aβ-stimulated luciferase activity of the 7-kb iNOS-LUC promoter construct (Fig. 5*B*)

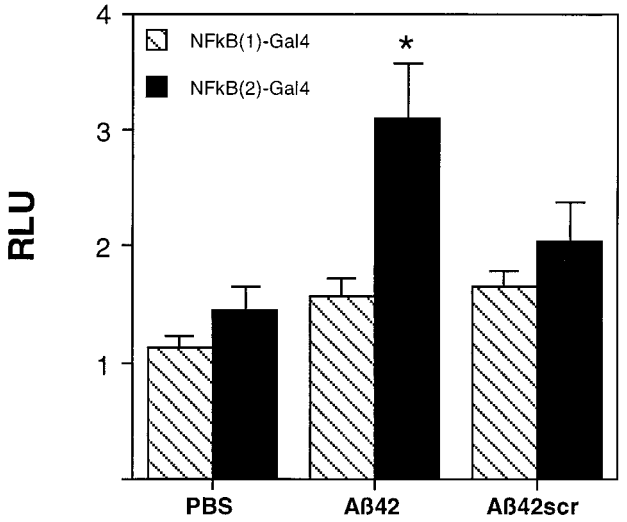

FIG. 4. Aβ42 activates NFκB at p65/RelA TAD 2. NFκB(1)-Gal4 and NFκB(2)-Gal4 expression constructs containing the first and second TADs of p65/RelA, respectively, were individually cotransfected with the yeast Gal4-UAS luciferase reporter plasmid to determine from which domain NFκB activation by Aβ42 occurred. Ten micromolar Aβ42-stimulated astrocytes showed approximately 2- to 3-fold more NFκB(2)-Gal4 luciferase activity compared with PBS-treated or 10 μM Aβ42scr-treated cells. There was no significant stimulation of NFκB(1)-Gal4 in Aβ42-treated cells compared with PBS-treated or 10 μM Aβ42scr-treated cells. *, Significantly different from PBS control ($P < 0.005$).

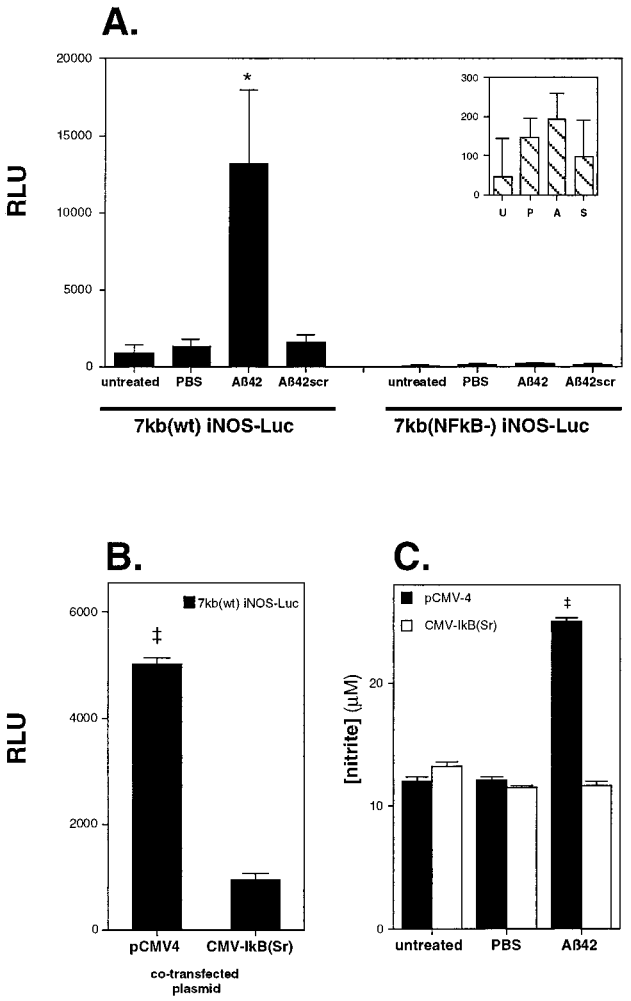

FIG. 5. Aβ42 stimulates iNOS in astrocytes in an NFκB-dependent manner. (*A*) Aβ42-stimulated iNOS promoter activity as determined by luciferase activity. Astrocytes were transfected with the 7-kb iNOS promoter luciferase reporter construct [7kb(wt) iNOS-LUC] and then either left untreated or stimulated by PBS, 10 μM Aβ42, or 10 μM Aβ42scr for 12 hr. Only Aβ42 significantly stimulated iNOS promoter activity. Inactivation of the TATAA-box proximal NFκB response element in the 7-kb iNOS promoter by site-directed mutagenesis [7kb(NFκB$^-$) iNOS-LUC] results in no significant promoter activity by Aβ42. (*Inset*) The same 7kb(NFκB$^-$) iNOS-LUC RLU data with a more focused ordinate range. U, P, A, and S are untreated, PBS-, Aβ42-, and Aβ42scr-treated cells, respectively. Data (mean RLU ± SEM) represent n = 8 transfections. (*B*) Cotransfecting the 7-kb iNOS-LUC construct with CMV-IκB(Sr) reduced Aβ-stimulated iNOS promoter activity to near background levels compared with cotransfection of 7kb(wt) iNOS-LUC with the backbone vector pCMV4. Data (mean RLU ± SEM) represent n = 6 transfections. (*C*) iNOS activity was determined by measuring the production of nitrite by a modified Griess assay as described. Aβ42-stimulated nitrite production was reduced to background control levels in astrocytes transfected with CMV-IκB(Sr), but not in Aβ42-stimulated astrocytes transfected with backbone vector pCMV4 alone. (Each transfection well received a total of 750 ng of plasmid DNA. Control backbone vector transfection wells received 750 ng of pCMV4 and CMV-IκB(Sr) transfection wells received 0.75 ng of CMV-IκB(Sr) plus 749.25 ng of pCMV4.) Data (mean ± SEM) represent n = 11 transfections. ∗, Significantly different from PBS control ($P < 0.05$); ‡, significantly different from CMV-IκB(Sr) ($P < 0.005$).

and NO production, as measured by the stable metabolites nitrite and nitrate (Fig. 5*C*). These three approaches demonstrate that Aβ42 stimulation of iNOS expression and NO production is NFκB-dependent.

DISCUSSION

We report here that the neurotoxic 42-aa Aβ peptide stimulates the activation of the transcription factor NFκB in cultured rat astrocytes in a dose-dependent manner, whereas a scrambled-sequence Aβ42 peptide at an equal concentration does not. Although expression of all five NFκB/Rel proteins can be detected in astrocytes, only specific Rel family members (p50 and p65/RelA) participate in Aβ activation. Moreover, Aβ42 stimulation of NFκB occurs selectively from TAD 2 of p65/RelA and not from TAD 1. Last, Aβ42 stimulation of iNOS gene expression and NO production is almost completely NFκB dependent.

Nitrogen species such as NO and NO-derived peroxynitrite are strong inducers of oxidative stress. It is therefore important to understand the molecular mechanisms underlying NO activation in an attempt to slow or prevent oxidative injury to the brain. This is emphasized by initial studies on dementia onset and the use of anti-inflammatory drugs and antioxidants (30–32). Chronic antioxidant usage, which may curb oxidative damage to cells, appears to result in a delay of dementia in AD patients. A prominent source of the oxidative damage seen in AD is peroxynitrite (16). Our results are consistent with previous studies that have shown that iNOS expression and peroxynitrite damage occur throughout the AD brain (8), and that NFκB activation can be observed in AD brain sections (21). However, our data couple Aβ42-stimulated NFκB activation in AD to the production of iNOS and NO. These studies provide direct support for the postulation (33) of a neurotoxic role for NFκB in AD in the context of glia and suggest that in AD, NFκB is not "protective" in glia as it can be in neurons (34). These studies also provide a model for how glia participate in the oxidative damage widely seen in AD and allow a focus on specific signaling pathways involving p65/RelA. Aβ42 exposure likely influences multiple signal transduction pathways, some of which ultimately can lead to enhanced NO production and subsequent oxidative damage. It should also be noted that other Aβ42-stimulated signal transduction pathways not involving NFκB or NO may lead to oxidative injury. Nevertheless, our data, which strongly implicate TAD 2 of NFκB p65/RelA in the induction of NO production by Aβ42 and therefore potential oxidative injury to the brain, may provide new therapeutic approaches to AD.

We thank the laboratory of Dr. D. Martin Watterson for assistance with peptide production and characterization. These studies were supported in part by National Institutes of Health Grants AG13939 and GM30861.

1. Masliah, E., Sisk, A., Mallory, M., Mucke, L., Schenk, D. & Games, D. (1996) *J. Neurosci.* **16,** 5796–5811.
2. Hsiao, K., Chapman, P., Nilsen, S., Eckman, C., Harigaya, Y., Younkin, S., Yang, F. & Cole, G. (1996) *Science* **274,** 99–102.
3. Selkoe, D. J. (1991) *Neuron* **6,** 487–498.
4. Griffin, W. S. T. & Stanley, L. C. (1993) in *Biology and Pathology of Astrocyte-Neuron Interactions*, ed. Federoff, S. (Plenum, New York), pp. 359–381.
5. Mrak, R. E., Sheng, J. G. & Griffin, W. S. T. (1995) *Human Pathol.* **26,** 816–823.
6. Hu, J., Akama, K. T., Krafft, G. A., Chromy, B. A. & Van Eldik, L. J. (1998) *Brain Res.* **785,** 195–206.
7. Wallace, M. N., Geddes, J. G., Farquhar, D. A. & Masson, M. R. (1997) *Exp. Neurol.* **144,** 266–272.
8. Smith, M. A., Richey-Harris, P. L., Sayre, L. M., Beckman, J. S. & Perry, G. (1997) *J. Neurosci.* **17,** 2653–2657.
9. Mattson, M. P. (1997) *Alzheimer's Disease Rev.* **2,** 1–14.
10. Hensley, K., Butterfield, D. A., Hall, N., Cole, P., Subramaniam, R., Mark, R., Mattson, M. P., Markesbery, W. R., Harris, M. E., Aksenov, M., Aksenova, M., Wu, J. F. & Carney, J. M. (1996) *Ann. N.Y. Acad. Sci.* **34,** 120–134.
11. Van Dyke, K. (1997) *Med. Hypotheses* **48,** 375–380.
12. Rossi, F. & Bianchini, E. (1996) *Biochem. Biophys. Res. Commun.* **225,** 474–478.

13. Meda, L., Cassatella, M. A., Szendrei, G. I., Otvos, L., Baron, P., Villalba, M., Ferrari, D. & Rossi, F. (1995) *Nature (London)* **374,** 647–650.
14. Goodwin, J. L., Uemura, E. & Cunnick, J. E. (1995) *Brain Res.* **692,** 207–214.
15. Ii, M., Sunamoto, M., Ohnishi, K. & Ichimori, Y. (1996) *Brain Res.* **720,** 93–100.
16. Beckman, J. S. & Koppenol, W. H. (1996) *Am. J. Physiol.* **271,** C1424–C1437.
17. Xie, Q., Kashiwabara, Y. & Nathan, C. (1994) *J. Biol. Chem.* **269,** 4705–4708.
18. Thanos, D. & Maniatis, T. (1995) *Cell* **80,** 529–532.
19. Nunokawa, Y., Ishida, N. & Tanaka, S. (1994) *Biochem. Biophys. Res. Commun.* **200,** 802–807.
20. O'Neill, L. A. J. & Kaltschmidt, C. (1997) *Trends Neurosci.* **20,** 252–258.
21. Terai, K., Matsuo, A., McGeer, E. G. & McGeer, P. L. (1996) *Brain Res.* **739,** 343–349.
22. Hu, J., Castets, F., Guevara, J. L. & Van Eldik, L. J. (1996) *J. Biol. Chem.* **271,** 2543–2547.
23. Andrews, N. C. & Faller, D. V. (1991) *Nucleic Acids Res.* **19,** 2499.
24. Fujita, T., Shibuya, H., Hotta, H., Yamanishi, K. & Taniguchi, T. (1987) *Cell* **49,** 357–367.
25. Brockman, J. A., Scherer, D. C., McKinsey, T. A., Hall, S. M., Qi, X., Lee, W. Y. & Ballard, D. W. (1995) *Mol. Cell. Biol.* **15,** 2809–2818.
26. deVera, M. E., Shapiro, R. A., Nussler, A. K., Mudgett, J. S., Simmons, R. L., Morris, S. M., Jr., Billar, T. R. & Geller, D. A. (1996) *Proc. Natl. Acad. Sci. USA* **93,** 1054–1059.
27. Watanabe, G., Howe, A., Lee, R. J., Albanese, C., Shu, I.-W., Karnezis, A. N., Zon, L., Kyriakis, J., Rundell, K. & Pestell, R. G. (1996) *Proc. Natl. Acad. Sci. USA* **93,** 12861–12866.
28. Schmitz, M. L., dos Santos Silva, M. A. & Baeuerle, P. A. (1995) *J. Biol. Chem.* **270,** 15576–15584.
29. Seipel, K., Georgiev, O. & Schaffner, W. (1992) *EMBO J.* **11,** 4961–4968.
30. Breitner, J. C. (1996) *Annu. Rev. Med.* **47,** 401–411.
31. Sano, M., Ernesto, C., Thomas, R. G., Klauber, M. R., Schafer, K., Grundman, M., Woodbury, P., Growdon, J., Cotman, C. W., Pheiffer, E., Schneider, L. S. & Thal, L. J. (1997) *N. Engl. J. Med.* **336,** 1216–1222.
32. Stewart, W. F., Kawas, C., Corrada, M. & Metter, E. J. (1997) *Neurology* **48,** 626–632.
33. Kaltschmidt, B., Uherek, M., Volk, B., Baeuerle, P. A. & Kaltschmidt, C. (1997) *Proc. Natl. Acad. Sci. USA* **94,** 2642–2647.
34. Barger, S. W., Horster, D., Furukawa, K., Goodman, Y., Krieglstein, J. & Mattson, M. P. (1995) *Proc. Natl. Acad. Sci. USA* **92,** 9328–9332.